Characterization details: Otsuka ELS Z particle analyzer was used to measure the hydrodynamic diameters of micelles. The morphology of the samples was observed under a field emission scanning electron microscope (FE-SEM, HITACHI SU-8000) and a transmission electron microscope (TEM, JEOL JEM-1210). The crystalline phases and crystalline degrees were measured by X-ray powder diffraction (XRD, SHIMADZU XRD-7000) analysis. X-ray photoelectron spectroscopy (XPS) spectra were taken using PHI Quantera SXM system equipped with an Al anode X-ray source. Thermogravimetric analysis (TGA) was carried out using a TG/DTA instrument (SEIKO-6300) at a heating rate of 10 °C·min^{-1} in air. The surface area of samples was measured by a N_2 adsorption/desorption isotherm.

Electrochemical measurement: Mesoporous TiO_2-RuO_2 composite was homogeneously mixed with a polyvinylidine difluoride (PVDF, 20 wt%) in N-methylpyrolidinone solvent. The slurry was coated onto a graphite substrate. The electrodes were dried at 80 °C for 2 h in a vacuum oven. For comparison, mesoporous TiO_2 was also used. Each electrode contained 0.3 mg·cm^{-2} of electroactive material. The electrochemical measurements were conducted in a three-electrode electrochemical cell with a Pt counter electrode and Ag/AgCl as a reference electrode in a 0.5 M H_2SO_4 solution. The graphite substrate coated with mesoporous TiO_2-RuO_2 composite was used as the working electrode. Cyclic voltammetry measurements were obtained using an electrochemical workstation (CHI 660E CH Instruments, USA) in the scan range of 0.1 to 0.9 V.

Fig. S1

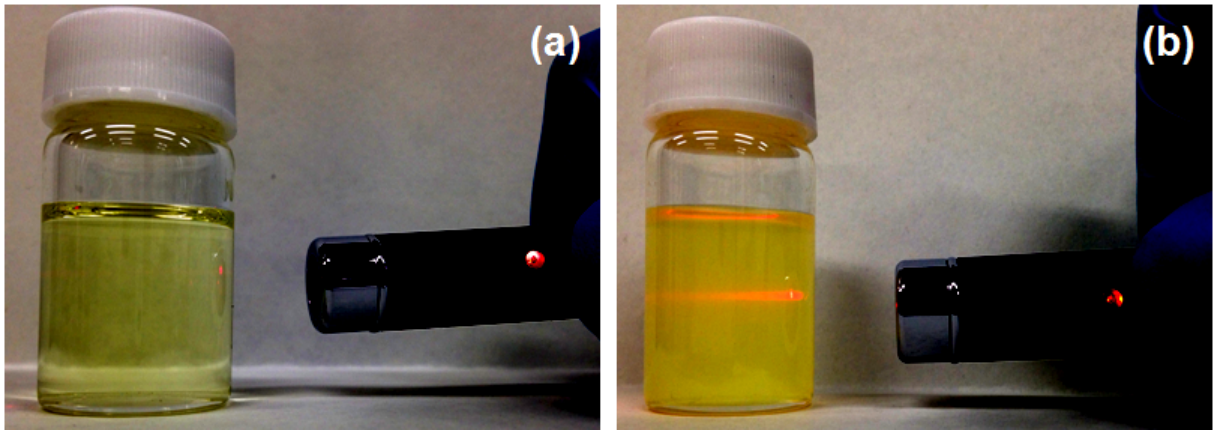

Fig. S1 Photographs of (a) PS-*b*-PVP-*b*-PEO solution dissolved in THF and (b) PS-*b*-PVP-*b*-PEO micellar solution after addition of HCl solution (Tyndall scattering is clearly confirmed).

Fig. S2

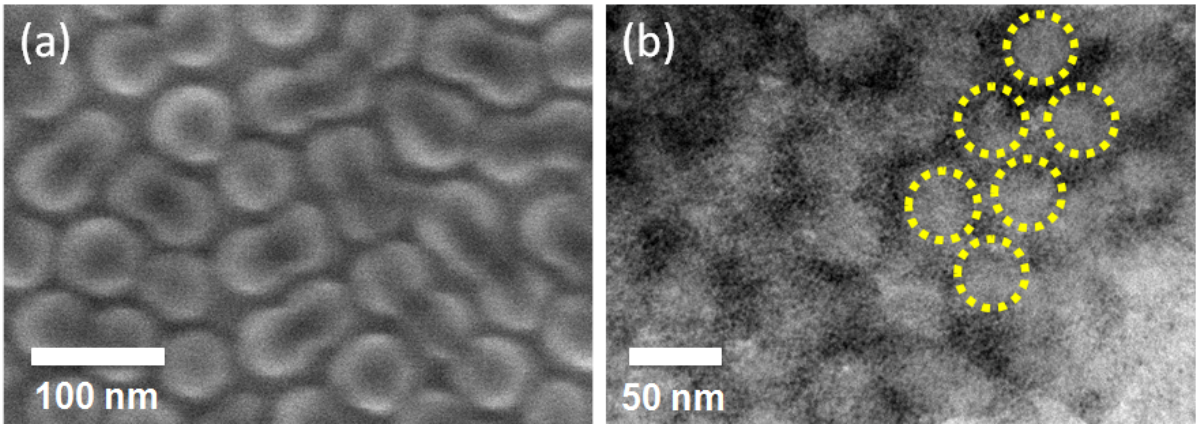

Fig. S2 (a) SEM and (b) TEM image of Ti/Ru/PS-*b*-PVP-*b*-PEO composite micelles. Yellow-colored circles indicate the shell region of inorganic precursors.

Fig. S3

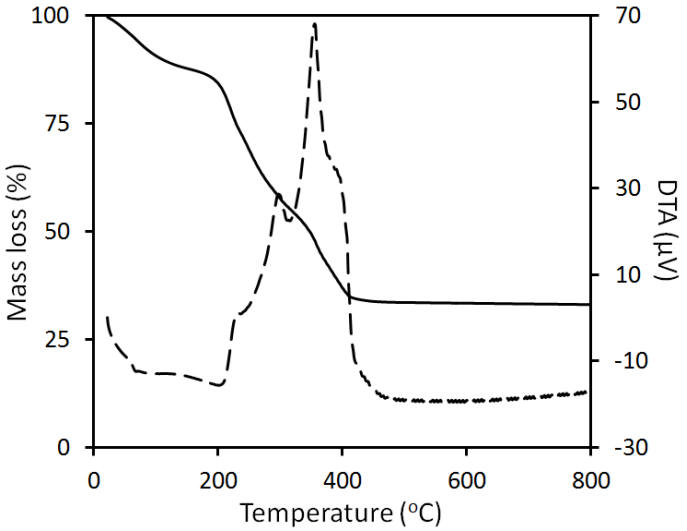

Fig. S3 Thermogravimetry/differential thermal analysis (TG/DTA) of Ti/Ru/PS-*b*-PVP-*b*-PEO composite micelles.

Fig. S4

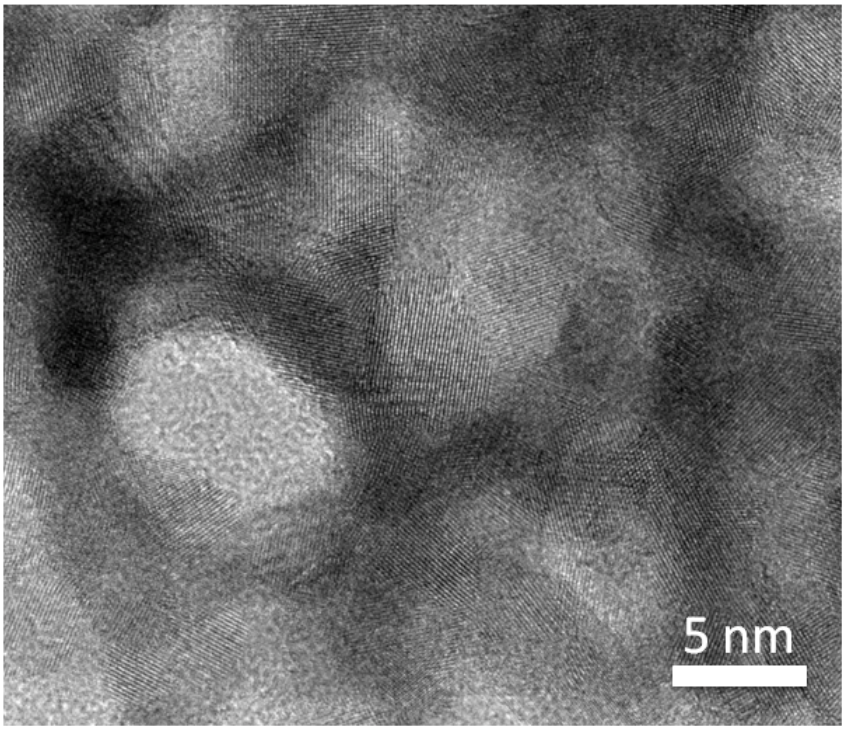

Fig. S4 HRTEM image of mesoporous TiO_2-RuO_2 composites.

Fig. S5

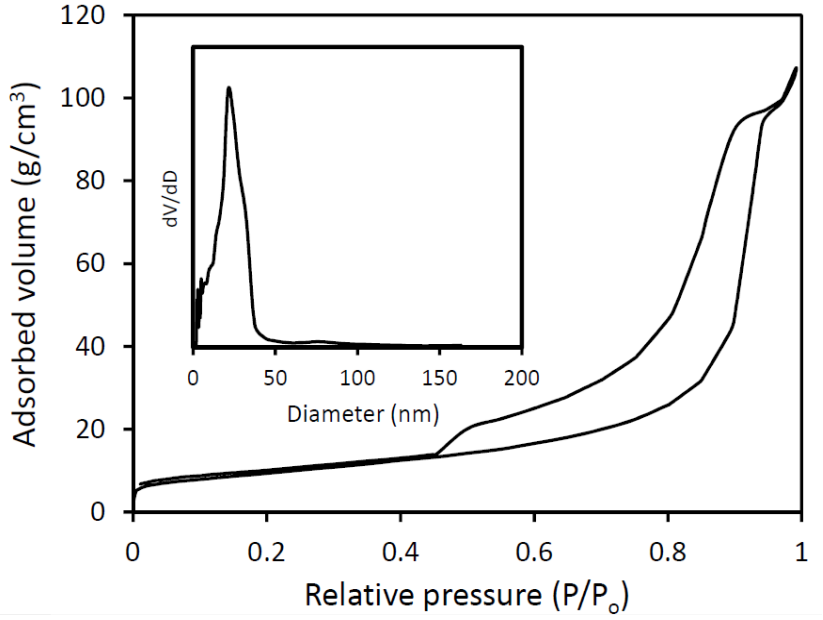

Fig. S5 N_2 adsorption-desorption isotherm of mesoporous TiO_2-RuO_2 composite. Pore size distribution is also shown in an inset figure.

Fig. S6

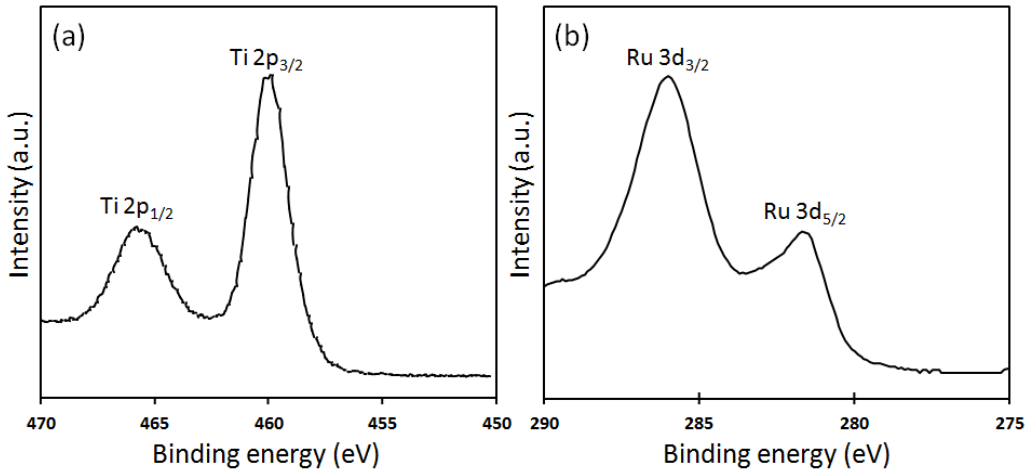

Fig. S6 XPS spectra (a) Ti 2p and (b) Ru 3d of mesoporous TiO_2-RuO_2 composite.

Fig. S7

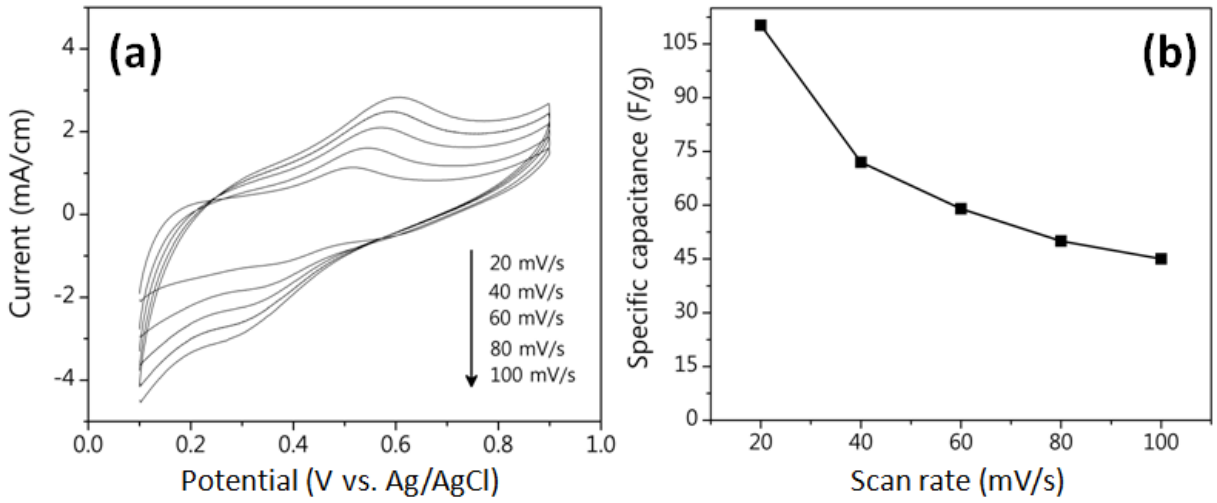

Fig. S7 (a) Cyclic voltammograms (CVs) of mesoporous TiO_2-RuO_2 composite at various scan rates and (b) effect of the scan rates on the capacitance performance.

Fig. S8

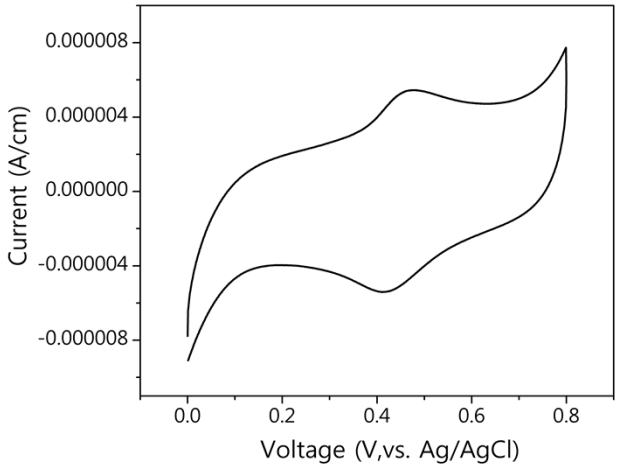

Fig. S8 Cyclic voltammogram (CV) of mesoporous TiO_2.